Rapid Communications | Editors' Suggestion

Nematic superconductivity in $Cu_{1.5}(PbSe)_5(Bi_2Se_3)_6$

Lionel Andersen, Zhiwei Wang, Thomas Lorenz, and Yoichi Ando*
Physics Institute II, University of Cologne, 50937 Köln, Germany

(Received 4 October 2018; revised manuscript received 29 November 2018; published 28 December 2018)

After the discovery of nematic topological superconductivity in $Cu_xBi_2Se_3$, carrier-doped topological insulators are established as a fertile ground for topological superconductors. The superconductor $Cu_{1.5}(PbSe)_5(Bi_2Se_3)_6$ (CPSBS) contains Bi_2Se_3 blocks as a constitutional unit, but its superconducting gap appears to have nodes [S. Sasaki *et al.*, Phys. Rev. B **90**, 220504 (2014)], which is in contrast to the fully opened gap in $Cu_xBi_2Se_3$ and the relation between the two superconductors remained an open question. Here, we report our observation of clear twofold symmetry in the in-plane magnetic field direction dependencies of the upper critical field and of the specific heat of CPSBS, where the direction of the maxima, which is different from that in $Cu_xBi_2Se_3$, indicates that the gap nodes are located in the mirror plane of the crystal lattice. This means that the topological nematic state with mirror-symmetry-protected nodes is realized in CPSBS.

DOI: 10.1103/PhysRevB.98.220512

The search for concrete materials to realize novel topological states of matter is an exciting frontier in condensed matter physics [1–3]. In that search, topological superconductors attract particular attention due to the potential appearance of exotic quasiparticles called Majorana fermions at their boundaries [2,4–7]. The superconductors derived from topological insulators (TIs) are expected to be a fertile ground in this respect, owing to the strong spin-orbit coupling which may give rise to an unconventional momentum-dependent superconducting gap even for the isotropic pairing force coming from conventional electron-phonon interactions [8,9].

The first of such materials was $Cu_xBi_2Se_3$ [10], which is synthesized by intercalating Cu into the van der Waals gap of the prototypical TI material Bi_2Se_3. $Cu_xBi_2Se_3$ shows superconductivity with $T_c \simeq 3$ K for $x \simeq 0.3$, and early point-contact spectroscopy measurements pointed to the occurrence of topological superconductivity associated with surface Majorana fermions [11]. Recent measurements of its bulk superconducting properties have elucidated [12,13] that it realizes a topological superconducting state which spontaneously breaks in-plane rotational symmetry in a twofold-symmetric manner, even though the crystal lattice symmetry is threefold. Such an unconventional state is consistent with one of the four possible superconducting states constrained by the D_{3d} lattice symmetry of Bi_2Se_3 [8,9]; this state, named the Δ_{4x} or Δ_{4y} state depending on the direction of nodes or gap minima, is characterized by a nematic order parameter and hence is called a *nematic superconducting state* [14]. It was reported that $Sr_xBi_2Se_3$ [15] and $Nb_xBi_2Se_3$ [16] also realize the nematic superconducting state [17–23].

An interesting superconducting compound related to $Cu_xBi_2Se_3$ is $Cu_x(PbSe)_5(Bi_2Se_3)_6$ (CPSBS), which was discovered in 2014 [24]. Its parent compound $(PbSe)_5(Bi_2Se_3)_6$ (PSBS) can be viewed as a natural heterostructure formed by a stack of two-quintuple-layer (QL) Bi_2Se_3 units alternating with one-bilayer PbSe units [25–29]. Since the binary compound PbSe is a topologically trivial insulator, PSBS consists of ultrathin TI layers separated by trivial-insulator layers. When Cu is intercalated into the van der Waals gap in the Bi_2Se_3 unit of PSBS, superconductivity with $T_c = 2.8$ K shows up and a nearly 100% superconducting volume fraction can be obtained for $x \simeq 1.5$. Since the structural unit responsible for superconductivity in CPSBS is essentially $Cu_xBi_2Se_3$, one would expect the same unconventional superconducting state to be realized in CPSBS. Nevertheless, there is a marked difference between the two compounds: Whereas there is strong evidence that CPSBS has gap nodes [24], $Cu_xBi_2Se_3$ is fully gapped [30]. Hence, it is important to clarify the nature of the nodal superconducting state in CPSBS.

In this Rapid Communication, we report our discovery of twofold symmetry in the upper critical field H_{c2} and the specific heat c_p in their dependencies on the magnetic field direction in the basal plane. The pattern of the twofold symmetry indicates that the gap nodes are lying in the mirror plane of the crystal, suggesting that the Δ_{4x} state with symmetry-protected nodes is realized in CPSBS. This is in contrast to the Δ_{4y} state realized in $Cu_xBi_2Se_3$, in which the nodes are not protected by symmetry and thus are lifted to form gap minima. We discuss that the likely cause of the Δ_{4x} state is the weak distortion of the Bi_2Se_3 lattice imposed by the PbSe units. This establishes CPSBS as a nematic topological superconductor with symmetry-protected nodes.

High-quality PSBS single crystals were grown by using a modified Bridgman method following Refs. [24,27]. X-ray Laue images were used for identifying the crystallographic *a* axis upon cutting the pristine crystals, which were then electrochemically treated to intercalate Cu following the recipe of Kriener *et al.* [31], and the superconductivity was activated by annealing. The precise *x* value determined by the weight change [31] was 1.47 for the two samples presented here. The superconducting shielding fraction (SF) of the samples was measured in a commercial superconducting quantum

*ando@ph2.uni-koeln.de

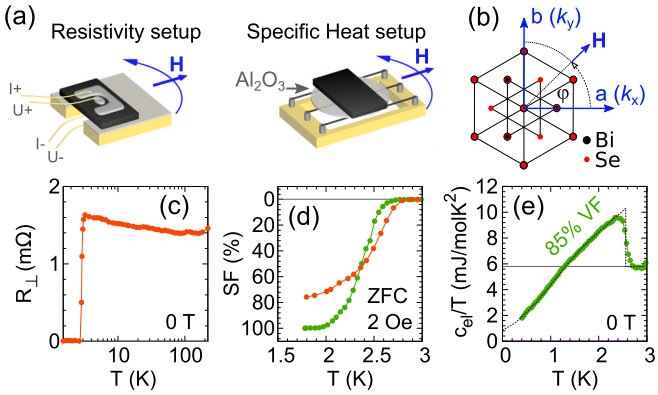

FIG. 1. (a) Schematic pictures of the setups to measure the in-plane magnetic field direction dependencies of the out-of-plane resistance $R_\perp$ and the specific heat c_p. (b) The monoclinic a axis of CPSBS lies in the mirror plane of the Bi_2Se_3 layers which nearly preserve the trigonal symmetry. (c) Temperature dependence of $R_\perp$ in sample A used for the resistive H_{c2} measurements. (d) The zero-field-cooled (ZFC) magnetization data showing shielding fractions of 75% and 104% in samples A (red) and B (green), respectively. (e) Temperature dependence of the electronic specific heat c_{el} in 0 T for sample B used for detailed $c_{el}(H)$ measurements; the solid line is the theoretical curve for a line-nodal superconducting gap [33] assuming a superconducting volume fraction of 85%. To facilitate the comparison with $Cu_xBi_2Se_3$, the molar volume is taken here for 1 mol of Bi_2Se_3.

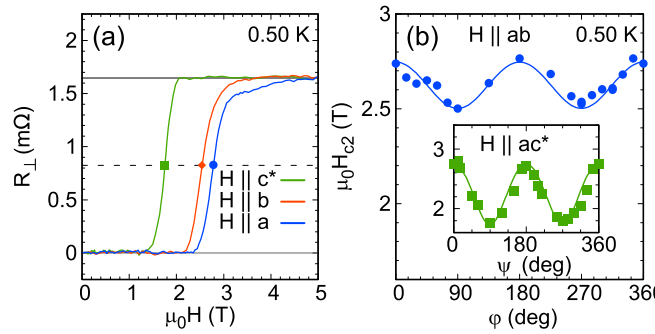

FIG. 2. (a) $R_\perp(H)$ curves measured for three principal directions of applied magnetic fields, showing a clear difference in H_{c2}. (b) Magnetic field direction dependencies of H_{c2} obtained from the $R_\perp(H)$ data in the in-plane rotation (main panel) and the out-of-plane rotation (inset); the angles φ and ψ are measured from the a axis.

interference device (SQUID) magnetometer. Further experimental details are given in the Supplemental Material [32].

To elucidate the possible in-plane anisotropy of the superconducting state, we employed the measurements of both the out-of-plane resistance $R_\perp$ and the specific heat c_p in various orientations of the in-plane magnetic field H [see Fig. 1(a) for configurations]. From the $R_\perp(H)$ data, the upper critical field H_{c2} was extracted by registering the field where 50% of the normal-state resistance is recovered. Note that $R_\perp$ measurements do not impose any in-plane anisotropy associated with the current direction. The c_p measurements were performed with a standard relaxation method using a home-built calorimeter [32] optimized for small heat capacities. Both measurements were done in a split-coil magnet with a ^{3}He insert (Oxford Instruments Heliox), with which the magnetic field direction with respect to the sample holder can be changed with a high accuracy ($\pm1^\circ$) by rotating the insert in the magnet. With a manual second rotation axis on the cold finger, measurements with H rotating in either the ab or ac^* plane were possible (note that $\vec{c}^* \parallel \vec{a} \times \vec{b}$ [27,32]). We estimate the possible misalignment of the magnetic field to be $\pm2^\circ$. The two samples used for measuring $R_\perp$ and c_p shown here presented the SF of 75% and 104%, respectively [Fig. 1(d)]. Here, no demagnetization correction is applied, since the magnetic field was applied parallel to the wide face of the platelet-shaped samples so that the demagnetization factor was >0.95.

The temperature dependence of $R_\perp$ presents a weak upturn below $\sim$100 K [Fig. 1(c)], which reflects the quasi-two-dimensional (2D) electronic states of CPSBS. The $R_\perp(H)$ curves measured at 0.5 K with the applied magnetic field in the three orthogonal directions, a, b, and c^* axes, are shown in Fig. 2(a). One can immediately see that H_{c2} for the three magnetic field directions are different; the smallest value for $H \parallel c^*$ is a consequence of the quasi-2D nature and was already reported [24], but here we observe that there is also an additional in-plane anisotropy between $H \parallel a$ and $H \parallel b$. The precise in-plane magnetic field direction dependence of H_{c2} at 0.5 K is shown in the main panel of Fig. 2(b), where one can see clear twofold symmetry with maxima at $H \parallel a$ and the variation $\Delta H_{c2}^{\parallel}$ of $\sim$0.25 T. As explained in detail in the Supplemental Material [32], the a axis in CPSBS is parallel to the mirror plane and hence the direction of H_{c2} maxima is 90° rotated from that in $Cu_xBi_2Se_3$ [13]. We note that anisotropic H_{c2} measurements with the current along the b axis were also performed, and H_{c2} was not affected by the current direction [32]. Also, the H_{c2} anisotropy in $R_\perp(H)$ was reproduced in one more sample [32].

For comparison, the magnetic field direction dependence of H_{c2} at 0.5 K in the ac^* plane is shown in the inset of Fig. 2(b), where the magnitude of the variation in H_{c2}, $\Delta H_{c2}^{\perp}$, is about 1.0 T. This $\Delta H_{c2}^{\perp}$ value means that, for the observed twofold in-plane anisotropy with $\Delta H_{c2}^{\parallel} \sim 0.25$ T to be ascribed to an accidental c^*-axis component of H, a sample misalignment of $\sim30^\circ$ would be necessary. This is obviously beyond the possible error in our experimental setup, and one can conclude that the twofold in-plane anisotropy is intrinsic.

Due to the volume sensitivity, the $c_p(T)$ data provide a better estimate of the superconducting volume fraction (VF) than the diamagnetic SF. After subtracting the phononic contribution [32], the electronic specific heat c_{el} shows a clear anomaly associated with the superconducting transition; Fig. 1(e) shows a plot of c_{el}/T vs T, which is fitted with a line-nodal gap theory [33] used for CPSBS in Ref. [24]. This fitting yields the superconducting VF of 85% for this sample, which is used for further c_{el} measurements.

The magnetic field dependencies of c_{el} at various temperatures for both $H \parallel a$ and $H \parallel b$ are shown in Fig. 3; the data presented here are after subtracting the Schottky anomaly [32] by using the same g-factor as that reported in Ref. [24]. One can see that at 2.01 and 1.01 K, c_{el} changes little above a

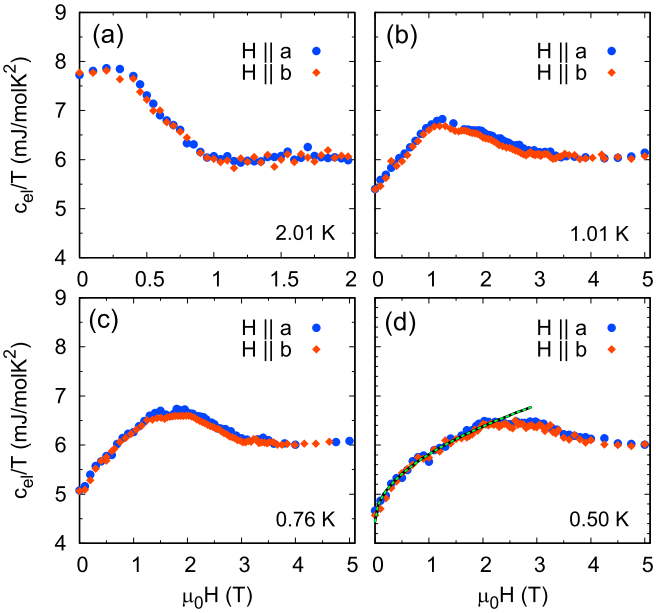

FIG. 3. Magnetic field dependencies of c_{el}/T at (a) 2.01 K, (b) 1.01 K, (c) 0.76 K, and (d) 0.50 K measured in $H \parallel a$ and $H \parallel b$. The dashed line in (d) shows the $\sqrt{H}$ behavior expected for a superconducting gap with line nodes, as was already reported in Ref. [24].

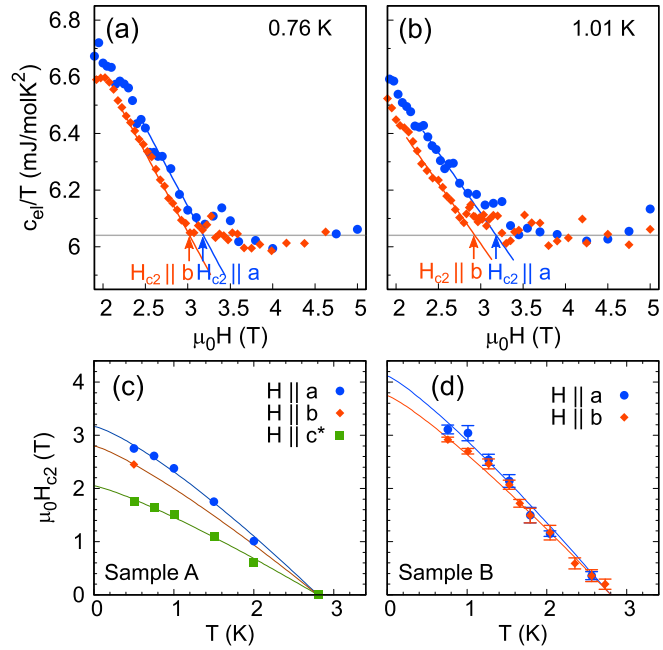

FIG. 4. (a), (b) Magnification of the $c_{el}(H)$ behavior near the H_{c2} at (a) 0.76 K and (b) 1.01 K for $H \parallel a$ and $H \parallel b$, showing how the H_{c2} values were extracted. (c), (d) Temperature dependencies of H_{c2} extracted from (c) the middle point in the $R_\perp(H)$ transitions in sample A and (d) disappearance of the superconducting contribution in c_{el} in sample B, for the principal magnetic field directions; the solid lines are fits to the empirical $\sim 1-(T/T_c)^{1.2}$ dependence.

certain H value, which we identify as H_{c2}. However, at lower temperature ($\lesssim$0.5 K) the change in the $c_{el}(H)/T$ behavior across H_{c2} becomes less evident and we lose the sensitivity to determine H_{c2}. As a result, the in-plane anisotropy in H_{c2} is best visible in c_{el} at intermediate temperatures around 1 K [Figs. 4(a) and 4(b)]. In our analysis of $c_{el}(H)$, H_{c2} was determined as the crossing point of the two linear fittings of the c_{el}/T vs H data below and above H_{c2} as shown in Figs. 4(a) and 4(b); here, one can see that the difference in H_{c2} for $H \parallel a$ and $H \parallel b$ is better discernible at 1.01 K with $\Delta H_{c2} \sim 0.34$ T than at 0.76 K. Importantly, H_{c2} is larger for $H \parallel a$, which is consistent with the result of the $R_\perp(H)$ measurements.

The temperature dependencies of H_{c2} extracted from $R_\perp(H)$ and $c_{el}(H)$ for the principal magnetic field orientations are plotted in Figs. 4(c) and 4(d), respectively. The absolute values of H_{c2} in the two panels are different, mainly because Fig. 4(c) shows the midpoint of the transition while Fig. 4(d) shows the complete suppression. Nevertheless, the in-plane anisotropy is consistently found in the $R_\perp(H)$ and $c_{el}(H)$ results. In Figs. 4(c) and 4(d), the $H_{c2}(T)$ data are fitted empirically with $H_{c2}(T) = H_{c2}(0)[1-(T/T_c)^a]$ with $a \approx 1.2$; the inapplicability of the conventional Werthamer-Helfand-Hohenberg theory for $H_{c2}(T)$ was already reported for CPSBS and was discussed to be a possible consequence of unconventional pairing [24].

To supplement the conclusion from H_{c2}, we have also measured the detailed magnetic field direction dependence of c_{el} at 0.76 and 1.01 K in various strengths of the in-plane magnetic field from 2.4 to 6.0 T [Figs. 5(a) and 5(b)]. One can clearly see twofold-symmetric variations where the maxima occur at $H \parallel a$ for $H < H_{c2}$, but the anisotropy quickly disappears for $H > H_{c2}$ [see also Fig. 5(c)]. This disappearance of the anisotropy in the normal state strongly supports the interpretation that the anisotropy is due to the nematicity which arises spontaneously in the superconducting state. It also demonstrates that the observed c_p anisotropy cannot be due to some g-factor anisotropy which might show up through the Schottky anomaly.

It is useful to note that in $Cu_xBi_2Se_3$, a sign change in the magnetic field direction dependence of c_{el} was observed [13]; namely, the maxima in c_{el} were observed for H normal to a mirror plane at high T and/or high H, but at low T and low H, c_{el} presented minima in this direction. Such a switching behavior was explained as a result of the competition between the Doppler-shift effect and the vortex-scattering effect discussed by Vorontsov and Vekhter (VV) [34]. According to VV, the latter effect is dominant at higher H at any temperature in a nodal superconductor and causes the maxima in c_{el} to appear for H in the nodal direction.

In view of the VV theory, the twofold in-plane anisotropy in CPSBS with maxima in c_{el} appearing for $H \parallel a$ near H_{c2} points to the realization of the Δ_{4x}-type superconducting gap, which has gap nodes in the mirror plane [see Fig. 5(d)]. This conclusion is different from that for $Cu_xBi_2Se_3$ [13], where the Δ_{4y} state is realized. Note that the direction of maxima in $H_{c2}(\varphi)$ [35] is also consistent with the Δ_{4x} gap in CPSBS and with the Δ_{4y} gap in $Cu_xBi_2Se_3$. While the Δ_{4x} state was originally predicted for the three-dimensional ellipsoidal Fermi surface of Bi_2Se_3 to have point nodes [8], the quasi-2D nature of the Fermi surface in CPSBS [28] extends the original

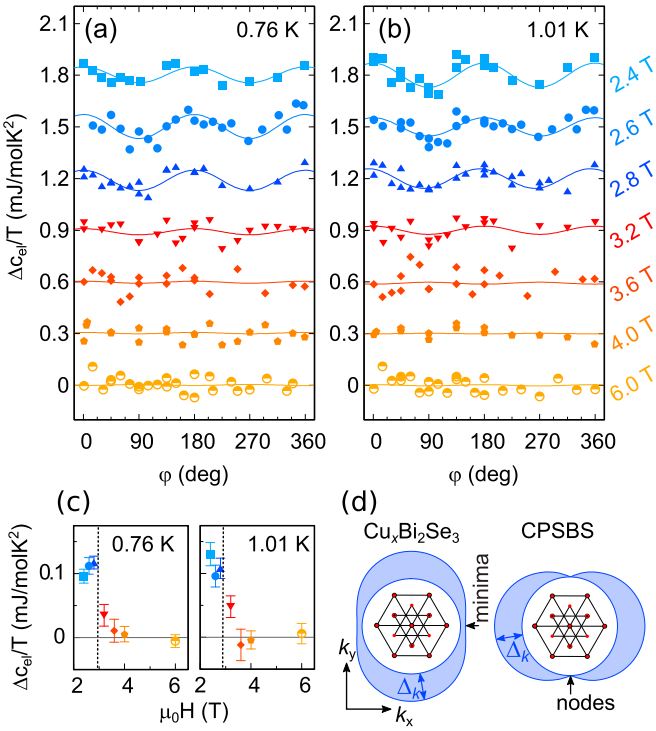

FIG. 5. (a), (b) Change in c_{el}/T as a function of the angle φ of the applied in-plane magnetic field at constant strengths of H across H_{c2} (2.4–6.0 T, the data are shifted for clarity) at 0.76 and 1.01 K, presenting twofold-symmetric oscillations at $H < H_{c2}$. (c) Dependence of the oscillation amplitude on the strength of H at 0.76 and 1.01 K, demonstrating its quick disappearance above H_{c2}. (d) Schematic pictures of the Δ_{4y} and Δ_{4x} gaps, which are realized in $Cu_xBi_2Se_3$ and CPSBS, respectively, in relation to the Bi_2Se_3 lattice.

point nodes into line nodes along the c^* direction, at least in the extreme 2D limit [36]. As pointed out by Fu [14], the nodes in the Δ_{4x} state are protected by mirror symmetry, which explains why CPSBS is a nodal superconductor despite its essential similarity to $Cu_xBi_2Se_3$.

It is useful to mention that the crystallographic symmetry of CPSBS belongs to the monoclinic space group $C2/m$ [26,27,29], which means that the lattice is actually twofold symmetric [37]. The monoclinic nature arises from the fact that PSBS is a heterostructure of two dissimilar crystal symmetries, the trigonal lattice of Bi_2Se_3 and the square lattice of PbSe (see Ref. [32] for details). The lowering of the symmetry makes one of the three equivalent mirror planes in Bi_2Se_3 to be the only mirror plane, which contains the monoclinic a axis; in fact, there is a weak but finite uniaxial distortion [32] in the Bi_2Se_3 QL units in PSBS [26,27]. According to the theory [14,35], under the constraint of the D_{3d} point group, an odd-parity superconducting state which breaks in-plane rotation symmetry must obey E_u symmetry and in general has a nematic gap function $\Delta(\mathbf{k}) = \eta_1\Delta_{4x} + \eta_2\Delta_{4y}$, where the two nodal gap functions Δ_{4x} and Δ_{4y} are degenerate and $\vec{\eta} = (\eta_1, \eta_2)$ can be viewed as the nematic director. This is why the E_u state is called nematic. However, for the physical properties to present a twofold anisotropy, a uniaxial symmetry-breaking perturbation is necessary [35]. In CPSBS, the weak uniaxial lattice distortion, which leads to the $C2/m$ symmetry, is apparently responsible for lifting the degeneracy between Δ_{4x} and Δ_{4y} and makes the nematic director take the definite direction $\vec{\eta} = (1, 0)$. Such a situation is rather similar to that realized in the high-T_c cuprate $YBa_2Cu_3O_y$, in which a tiny orthorhombic distortion dictates the orientation of the spontaneously formed nematic state [38], although the nematicity is about the normal state in $YBa_2Cu_3O_y$ while it is about the superconducting state in CPSBS.

We note that the ARPES measurements on superconducting CPSBS found no clear evidence for twofold-symmetric Fermi-surface distortion within the experimental error of ~2% [28]. Hence, the possible anisotropy in the Fermi velocity v_F cannot be large enough to directly account for the observed twofold anisotropy in H_{c2} of ~10%, but it must be responsible for lifting the degeneracy in the nematic state. The emerging picture is that the microscopic physics of electrons in doped Bi_2Se_3 chooses the E_u superconducting state to be the most energetically favorable, and then a symmetry-breaking perturbation sets the direction of $\vec{\eta}$, so that a twofold anisotropy shows up [39]. In this regard, there is a report that twofold anisotropy in $Sr_xBi_2Se_3$ correlates with a weak structural distortion [22]. Interestingly, the existence of gap nodes has been suggested for $Nb_xBi_2Se_3$ [40,41], which implies that the symmetry-breaking perturbation in $Nb_xBi_2Se_3$ is different from that in $Cu_xBi_2Se_3$ and prompts $\vec{\eta}$ to take (1,0).

In summary, we found that both the H_{c2} and the c_p of superconducting CPSBS present twofold-symmetric in-plane anisotropy with maxima occurring for $H \parallel a$. This points to the realization of the Δ_{4x}-type superconducting gap associated with symmetry-protected line nodes extending along the c^* direction. Hence, CPSBS is a nematic topological superconductor differing from $Cu_xBi_2Se_3$ in the orientation of the nematic director.

We thank T. Sato for reanalyzing the raw data of Ref. [28] to check for possible Fermi-surface anisotropy in CPSBS. We also thank Y. Vinkler-Aviv for helpful discussions about the point group. This work was funded by the Deutsche Forschungsgemeinschaft (DFG, German Research Foundation) Projects No. 277146847-A04 and No. 277146847-B01 – CRC 1238 (subprojects A04 and B01).

[1] M. Z. Hasan and C. L. Kane, Rev. Mod. Phys. **82**, 3045 (2010).
[2] X.-L. Qi and S.-C. Zhang, Rev. Mod. Phys. **83**, 1057 (2011).
[3] Y. Ando, J. Phys. Soc. Jpn. **82**, 102001 (2013).
[4] J. Alicea, Rep. Prog. Phys. **75**, 076501 (2012).
[5] C. W. J. Beenakker, Annu. Rev. Condens. Matter Phys. **4**, 113 (2013).
[6] S. R. Elliott and M. Franz, Rev. Mod. Phys. **87**, 137 (2015).
[7] M. Sato and Y. Ando, Rep. Prog. Phys. **80**, 076501 (2017).
[8] L. Fu and E. Berg, Phys. Rev. Lett. **105**, 097001 (2010).
[9] Y. Ando and L. Fu, Annu. Rev. Condens. Matter Phys. **6**, 361 (2015).

[10] Y. S. Hor, A. J. Williams, J. G. Checkelsky, P. Roushan, J. Seo, Q. Xu, H. W. Zandbergen, A. Yazdani, N. P. Ong, and R. J. Cava, Phys. Rev. Lett. **104**, 057001 (2010).

[11] S. Sasaki, M. Kriener, K. Segawa, K. Yada, Y. Tanaka, M. Sato, and Y. Ando, Phys. Rev. Lett. **107**, 217001 (2011).

[12] K. Matano, M. Kriener, K. Segawa, Y. Ando, and G.-q. Zheng, Nat. Phys. **12**, 852 (2016).

[13] S. Yonezawa, K. Tajiri, S. Nakata, Y. Nagai, Z. Wang, K. Segawa, Y. Ando, and Y. Maeno, Nat. Phys. **13**, 123 (2017).

[14] L. Fu, Phys. Rev. B **90**, 100509 (2014).

[15] Z. Liu, X. Yao, J. Shao, M. Zuo, L. Pi, S. Tan, C. Zhang, and Y. Zhang, J. Am. Chem. Soc. **137**, 10512 (2015).

[16] Y. Qiu, K. Nocona Sanders, J. Dai, J. E. Medvedeva, W. Wu, P. Ghaemi, T. Vojta, and Y. San Hor, arXiv:1512.03519.

[17] A. M. Nikitin, Y. Pan, Y. K. Huang, T. Naka, and A. de Visser, Phys. Rev. B **94**, 144516 (2016).

[18] Y. Pan, A. M. Nikitin, G. K. Araizi, Y. K. Huang, Y. Matsushita, T. Naka, and A. de Visser, Sci. Rep. **6**, 28632 (2016).

[19] J. Shen, W.-Y. He, N. F. Q. Yuan, Z. Huang, C.-w. Cho, S. H. Lee, Y. S. Hor, K. T. Law, and R. Lortz, npj Quantum Mater. **2**, 59 (2017).

[20] T. Asaba, B. J. Lawson, C. Tinsman, L. Chen, P. Corbae, G. Li, Y. Qiu, Y. S. Hor, L. Fu, and L. Li, Phys. Rev. X **7**, 011009 (2017).

[21] G. Du, Y. Li, J. Schneeloch, R. D. Zhong, G. Gu, H. Yang, H. Lin, and H.-H. Wen, Sci. China-Phys. Mech. Astron. **60**, 037411 (2017).

[22] A. Y. Kuntsevich, M. A. Bryzgalov, V. A. Prudkoglyad, V. P. Martovitskii, Y. G. Selivanov, and E. G. Chizhevskii, New J. Phys. **20**, 103022 (2018).

[23] M. P. Smylie, K. Willa, H. Claus, A. E. Koshelev, K. W. Song, W. K. Kwok, Z. Islam, G. D. Gu, J. A. Schneeloch, R. D. Zhong, and U. Welp, Sci. Rep. **8**, 7666 (2018).

[24] S. Sasaki, K. Segawa, and Y. Ando, Phys. Rev. B **90**, 220504 (2014).

[25] K. Nakayama, K. Eto, Y. Tanaka, T. Sato, S. Souma, T. Takahashi, K. Segawa, and Y. Ando, Phys. Rev. Lett. **109**, 236804 (2012).

[26] L. Fang, C. C. Stoumpos, Y. Jia, A. Glatz, D. Y. Chung, H. Claus, U. Welp, W.-K. Kwok, and M. G. Kanatzidis, Phys. Rev. B **90**, 020504 (2014).

[27] K. Segawa, A. Taskin, and Y. Ando, J. Solid State Chem. **221**, 196 (2015).

[28] K. Nakayama, H. Kimizuka, Y. Tanaka, T. Sato, S. Souma, T. Takahashi, S. Sasaki, K. Segawa, and Y. Ando, Phys. Rev. B **92**, 100508 (2015).

[29] H. Momida, G. Bihlmayer, S. Blügel, K. Segawa, Y. Ando, and T. Oguchi, Phys. Rev. B **97**, 035113 (2018).

[30] M. Kriener, K. Segawa, Z. Ren, S. Sasaki, and Y. Ando, Phys. Rev. Lett. **106**, 127004 (2011).

[31] M. Kriener, K. Segawa, Z. Ren, S. Sasaki, S. Wada, S. Kuwabata, and Y. Ando, Phys. Rev. B **84**, 054513 (2011).

[32] See Supplemental Material at http://link.aps.org/supplemental/10.1103/PhysRevB.98.220512 for supplemental data and discussions, which includes Refs. [42–46].

[33] H. Won and K. Maki, Phys. Rev. B **49**, 1397 (1994).

[34] A. Vorontsov and I. Vekhter, Phys. Rev. Lett. **96**, 237001 (2006).

[35] J. W. F. Venderbos, V. Kozii, and L. Fu, Phys. Rev. B **94**, 094522 (2016).

[36] T. Hashimoto, K. Yada, A. Yamakage, M. Sato, and Y. Tanaka, Supercond. Sci. Technol. **27**, 104002 (2014).

[37] The $C2/m$ symmetry is compatible with both the Δ_{4x} and Δ_{4y} gaps, which are derived from the E_u representation of the D_{3d} point group.

[38] Y. Ando, K. Segawa, S. Komiya, and A. N. Lavrov, Phys. Rev. Lett. **88**, 137005 (2002).

[39] In the normal state, there was no discernible in-plane anisotropy in the magnetoresistance, which is different from the case of $Sr_xBi_2Se_3$ reported in Ref. [22].

[40] M. P. Smylie, H. Claus, U. Welp, W. K. Kwok, Y. Qiu, Y. S. Hor, and A. Snezhko, Phys. Rev. B **94**, 180510 (2016).

[41] M. P. Smylie, K. Willa, H. Claus, A. Snezhko, I. Martin, W. K. Kwok, Y. Qiu, Y. S. Hor, E. Bokari, P. Niraula, A. Kayani, V. Mishra, and U. Welp, Phys. Rev. B **96**, 115145 (2017).

[42] L. E. Shelimova, O. G. Karpinskii, P. P. Konstantinov, E. S. Avilov, M. A. Kretova, G. U. Lubman, I. Y. Nikhezina, and V. S. Zemskov, Inorg. Mater. **46**, 120 (2010).

[43] J. P. Emerson, R. A. Fisher, N. E. Phillips, D. A. Wright, and E. M. McCarron, Phys. Rev. B **49**, 9256 (1994).

[44] K. A. Moler, D. L. Sisson, J. S. Urbach, M. R. Beasley, A. Kapitulnik, D. J. Baar, R. Liang, and W. N. Hardy, Phys. Rev. B **55**, 3954 (1997).

[45] C. Pérez Vicente, J. L. Tirado, K. Adouby, J. C. Jumas, A. A. Touré, and G. Kra, Inorg. Chem. **38**, 2131 (1999).

[46] T. Hahn, *International Tables for Crystallography*, Vol. A (International Union of Crystallography, Chester, U.K., 2005).